ELSEVIER

Fluid Dynamics Research 25 (1999) 315–333

FLUID DYNAMICS RESEARCH

# Numerical simulations of internal solitary waves with vortex cores

A. Aigner[a], D. Broutman[b], R. Grimshaw[a,*]

[a] *Department of Mathematics, Monash University, Clayton, VIC 3168, Australia*
[b] *School of Mathematics, UNSW, Sydney, NSW 2052, Australia*

Received 18 August 1998; received in revised form 16 November 1998; accepted 18 December 1998

**Abstract**

This paper deals with the numerical verification of the theory developed by Derzho and Grimshaw (DG) (1997, Phys. Fluids 9(11), 3378–3385) regarding solitary waves in stratified fluids with recirculation regions. The Boussinesq approximation is made and the stratification is chosen such that the Brunt-Väisälä frequency differs only slightly from uniform stratification. To establish the consistency of the numerical scheme the usual KdV and mKdV solutions are tested first and then the solutions obtained by DG are considered. It is found that these waves remain of permanent form and are stationary when viewed at their corresponding phase speed. The recirculation region remains stagnant to first order as predicted by DG. 

## 1. Introduction

Solitary wave propagation in stratified fluids may be characterized by the depth of the fluid, ranging from shallow to deep, and the magnitude of nonlinearity, which is related to the amplitude of the disturbance. Small amplitude disturbances are usually treated in a weakly nonlinear long wave approximation, typically leading to a Korteweg–de Vries type of equation for shallow fluids, or to the intermediate depth equation for deep fluids (see, for instance the recent review by Grimshaw, 1997).

Inclusion of higher-order terms in the asymptotic expansion enables the theory to be extended to larger amplitude disturbances. For instance Gear and Grimshaw (1983) have extended the theory for shallow fluids to second order. However, this amplitude expansion approach is generally not suitable for large amplitude waves, and in particular fails to generate solutions with vortex cores. Further, the analysis of Pelinovsky and Grimshaw (1997) indicates that solitary waves of large amplitudes may be unstable, and evolve into structures with vortex cores.

* Corresponding author. Tel.: 61-3-905.4458; fax: 61-3-905.3870/4403; e-mail: rhjg@wave.maths.monash.edu.au.

0169-5983/99/$ - see front matter 
PII: S0169-5983(98)00046-X

The study of steady internal waves is most accessible through the Dubreil–Jacotin–Long equation (Dubreil-Jacotin, 1937; Long, 1953), which we will denote as Long's equation as is customary. Long's equation is applicable for the study of steady solitary waves in a stratified, incompressible and inviscid fluid, when the solution has no closed streamlines, and there is no upstream influence on the flow.

Long's equation is linear for uniform stratification in the Boussinesq approximation yielding an equation similar to that for linear waves (Chan et al., 1982; Leonov and Miropol'skiy, 1975). It follows that solitary waves are then precluded. While for incompressible fluids and constant $N$ the Boussinesq approximation removes the existence of solitary waves, Long and Morton (1966) and Grimshaw (1980/81) have shown, that on one hand allowance of the slightest compressibility makes solitary waves possible. On the other hand, a small departure from the Boussinesq approximation, or a small departure from uniform stratification again make solitary waves possible (see, for instance, Benney and Ko, 1978; Grimshaw and Yi, 1991). We make the latter choice here.

For a fluid of finite depth with rigid top and bottom boundaries, the absence of recirculation regions limits Long's equation to the study of waves of amplitudes less than a critical amplitude $A_*$, for which a stagnation point is situated at the upper boundary for a wave of depression (and at the lower boundary for a wave of elevation). Note that we consider waves of depression henceforth; waves of elevation are analogous. For amplitudes greater than $A_*$ a vortex will be generated near the upper boundary.

The appearance of closed streamlines terminates the strict validity of solutions to Long's equation, but Derzho and Grimshaw (DG) (1997) have shown that the range of solitary wave solutions of Long's equation can be extended to solutions possessing vortex cores. The usual solitary wave solution valid in the outer region is matched to another solution in the inner region, thereby extending the study of solitary waves to amplitudes in excess of $A_*$. To achieve this, it is necessary to include a small vortex core region near the upper boundary, in which the flow is stagnant to leading order. The solutions so obtained exhibit amplitude-width relationships characteristic for observed large amplitude waves, which are known to possess closed streamlines and a pocket of recirculating flow; the width of the disturbance increases with amplitude.

The aim of this paper is to verify the existence and permanence of such asymptotic solutions by solving the time-dependent governing equations over a long period. The outline of this paper is as follows. In Section 2 the governing equations are derived and in Section 3 the steady asymptotic solutions are obtained. In Sections 4 and 5 the results and conclusions are stated.

## 2. Governing equations

Consider a two-dimensional inviscid incompressible fluid of undisturbed depth $h$, with rigid upper and lower boundaries. The governing equations are,

$$\rho\{u_t + \boldsymbol{u}\cdot\nabla u\} = -p_x, \tag{1}$$

$$\rho\{w_t + \boldsymbol{u}\cdot\nabla w\} = -p_z - \rho g, \tag{2}$$

$$\rho_t + \boldsymbol{u}\cdot\nabla\rho = 0, \tag{3}$$

$$\nabla\cdot\boldsymbol{u} = 0 \tag{4}$$

where $\boldsymbol{u}=(u,w)$ is the velocity vector, $p$ the pressure, $\rho$ the total density and the cartesian coordinate system is orientated such that the $x$-axis is horizontal and the $z$-axis points vertically upward. We introduce a streamfunction $\psi$, with $u=-\psi_z$ and $w=\psi_x$, such that the continuity equation (4) is identically satisfied.

Next we chose a reference frame moving with the wave in the positive $x$-direction at the phase speed $c$. Thus, let

$$s=x-c\,t, \tag{5}$$

and introduce a modified streamfunction $\phi(s,z)$ by

$$\psi(s,z)=-c\,z+\phi(s,z). \tag{6}$$

The conservation of density equation (3) for steady flow then implies that

$$\rho=\rho(\phi). \tag{7}$$

Elimination of the pressure between the momentum equations (1) and (2) and making use of the transformation (5)–(7) yields a single equation for the streamfunction $\phi$:

$$J\left[\phi_{ss}+\phi_{zz}+\frac{1}{\rho}\frac{\mathrm{d}\rho}{\mathrm{d}\phi}\left(gz+\frac{1}{2}(\phi_s^2+\phi_z^2)\right),\phi\right]=0,$$

where $J$, the Jacobian operator, is given by $J(A,B)=A_s B_z-A_z B_s$.

It follows that for a vorticity function $\mathscr{G}(\phi)$, determined from upstream conditions, the streamfunction $\phi$ has to satisfy the following nonlinear equation, derived by Dubreil-Jacotin (1937) and Long (1953):

$$\phi_{ss}+\phi_{zz}+\frac{1}{\rho}\frac{\mathrm{d}\rho}{\mathrm{d}\phi}\left(g\,z+\frac{1}{2}(\phi_s^2+\phi_z^2)\right)=\mathscr{G}(\phi). \tag{8}$$

Note that Long's equation assumes all streamlines originate upstream. The function $\mathscr{G}$ can be obtained on those streamlines originating upstream, where we assume that $\psi\to 0$, so that

$$\phi\to c\,z, \tag{9}$$

$$\rho\to\bar{\rho}(z), \tag{10}$$

where $\bar{\rho}(z)$ is the basic density profile. It follows that

$$\rho(\phi)=\bar{\rho}(\phi/c), \tag{11}$$

$$\mathscr{G}(\phi)=\frac{1}{\rho}\frac{\mathrm{d}\rho}{\mathrm{d}\phi}\left(\frac{g\,\phi}{c}+\frac{1}{2}c^2\right). \tag{12}$$

Introduction of dimensionless coordinates based on the height of undisturbed fluid $h$ and the phase speed $c$,

$$\phi'=\frac{\phi}{c\,h},\qquad s'=\frac{s}{h},\qquad z'=\frac{z}{h} \tag{13}$$

and considering a basic density field close to uniform stratification

$$\bar{\rho}(z')=\rho_0(1-\sigma z'-\sigma^2 f(z')) \tag{14}$$

yields for Eq. (8) after omitting the prime superscripts

$$\phi_{ss} + \phi_{zz} + \lambda(\phi - z)(1 + \sigma f_{\phi}(\phi) + \sigma\phi) - \tfrac{1}{2}\sigma(\phi_s^2 + \phi_z^2 - 1) + \mathrm{O}(\sigma^2) = 0, \tag{15}$$

where

$$\lambda = \sigma g h / c^2. \tag{16}$$

$\lambda$ is an inverse Froude number, and scales with unity with respect to the small parameter $\sigma$, which characterizes the weak stratification.

If the Boussinesq approximation is made Eq. (8) reduces to

$$\phi_{ss} + \phi_{zz} + \frac{1}{\rho_0}\frac{\mathrm{d}\rho}{\mathrm{d}\phi} g z = \mathscr{G}(\phi) \tag{17}$$

and Eq. (15) becomes

$$\phi_{ss} + \phi_{zz} + \lambda(\phi - z)(1 + \sigma f_{\phi}(\phi)) + \mathrm{O}(\sigma^2) = 0, \tag{18}$$

where the term $\phi f_{\phi}(\phi)$ constitutes the only nonlinearity of Long's equation to this order in $\sigma$. This indicates that for linear stratification Long's equation is linear, prohibiting the existence of solitary waves. The boundary conditions are:

$$\phi_x = 0 \quad \text{on} \quad z = 0, 1, \tag{19}$$

$$\phi \sim z \quad \text{as} \quad x \to \pm\infty. \tag{20}$$

Eqs. (18)–(20) provide a complete formulation of the problem if all streamlines originate upstream, thereby excluding the possible presence of a recirculation region. Derzho and Grimshaw (1997) have shown that a recirculation region can be incorporated by assuming that inside of this region $\rho$ is constant and then the vorticity equation (8) reduces to

$$\phi_{ss} + \phi_{zz} = g(\phi)$$

inside of this region, where $g$ is a function of $\phi$ yet to be determined.

## 3. Derivation of the steady solitary wave solutions

While DG derive a solution from (15) without necessarily making the Boussinesq approximation, we will exploit the Boussinesq approximation here. The following derivation will therefore parallel the derivation given in DG and can be obtained directly by taking the Boussinesq limit of the solution given by DG. Solitary wave solutions are sought, whose width is much greater than the channel depth. We introduce the stretched variable $X = \varepsilon s$, and let the stratification parameter $\sigma$ scale with $\varepsilon^2$. An asymptotic expansion of $\phi$ and $\lambda$ in terms of $\varepsilon^2$

$$\phi(X, z) \sim \sum_{k=0}^{\infty} \varepsilon^{2k} \phi^k(X, z), \tag{21}$$

$$\lambda \sim \sum_{k=0}^{\infty} \varepsilon^{2k} \lambda^k, \tag{22}$$

when substituted into (18) yields the equation

$$\phi^0_{zz} + \lambda^0(\phi^0 - z) = 0$$

for the zeroth order, which has to satisfy the boundary conditions (19) and (20) giving

$$\phi^0 = z + A(X)\sin(\pi z), \tag{23}$$

$$\lambda^0 = \pi^2, \tag{24}$$

where only the first vertical mode is considered here. At the next order in the expansion one gets

$$\phi^1_{zz} + \pi^2\,\phi^1 + F^1 = 0, \quad F^1 = A_{XX}W + \lambda^1 AW + \pi^2 AW f_\phi(\phi^0),$$

where $W = \sin(\pi z)$, from which an amplitude equation is determined by exploiting the appropriate compatibility condition,

$$\int_0^1 F^1 W\,\mathrm{d}z = 0, \tag{25}$$

yielding the following equation for $A$:

$$A_{XX} + \lambda^1 A + M(A) = 0, \tag{26}$$

where [1]

$$M(A) = 2\pi^2 \int_0^1 A\sin^2(\pi z) f_\phi(z + A\sin(\pi z))\mathrm{d}z. \tag{27}$$

Eq. (26) can be integrated once to give

$$A_X^2 + \lambda^1 A^2 + 2\int_0^A M(A')\mathrm{d}A' = 0. \tag{28}$$

It is clear now that if $f(z') = 0$, corresponding to linear stratification, Eq. (26) is linear.

For amplitudes greater than $A_* = 1/\pi$ a recirculation region is generated in which the flow reverses, since then $\phi^0_z$ can change sign. This amplitude is reached at the upper boundary for a wave of depression. The flow field is now divided into three regions, an outer region where Eqs. (26) and (18) hold, an inner region and a recirculation core which are discussed next. Assuming the width of the inner solution is large compared to the depth and the amplitude is close to $A_*$, the solution in the inner region is

$$A(\xi) = A_* + \mu B(\xi) \quad \text{with } 0 \leqslant B(\xi) \leqslant 1, \tag{29}$$

where $\xi = \beta s$ is another stretched variable. Clearly $\varepsilon \ll \beta$ and then $\mu\beta^2 = \varepsilon^2$, so that the width of the inner zone is smaller than the total length scale of the wave and tends to zero as $\mu \to 0$. In order to derive an approximative governing equation for the inner solution the depth of the vortex core $\eta$ is assumed small, $\eta = \delta F(\xi)$, where $\delta$ is another small parameter and $F(\xi)$ is a function describing the shape of the vortex boundary (i.e. the vortex core is given by $z = 1 - \eta$ for $|\xi| < \xi_0$, where $\xi_0$ is yet to be determined). It is shown by DG that an optimal balance of parameters occurs when

[1] Note that $M(A)$ has the correct factor $2\pi^2$, cf. Eq. (31) in Derzho and Grimshaw (1997).

$\delta=\varepsilon^{2/3}$, $\beta=\varepsilon^{1/3}$ and $\mu=\varepsilon^{4/3}$. Substituting (29) into the first-order equations and using a compatibility condition similar to (25) yields an approximative governing equation in terms of $B(\xi)$,

$$B_{\xi\xi}+\lambda^1 A_*+M(A_*)+2\pi\phi^1(\xi,1)=0, \tag{30}$$

where the boundary $z=1-\eta$ was relocated asymptotically to $z=1$. The unknown term $\phi^1(\xi,1)$ can be obtained, using the fact that $\phi$ and the pressure have to be continuous across the vortex core boundary, so that Eq. (30) becomes

$$B_\xi^2=R(A_*)[1-B]-\frac{8v}{15}[1-B^{5/2}], \tag{31}$$

where

$$R(A_*)=2M(A_*)-\frac{4}{A_*}\int_0^{A_*}M(A')\,\mathrm{d}A' \quad \text{and} \quad v=(2\pi\mu)^{3/2}/\varepsilon^2. \tag{32}$$

Inside the recirculation core the key assumption is that the flow is stagnant to leading order, i.e. the vorticity is $0(\sigma)$ in the core. For a nontrivial solution to exist the right-hand side of (31) must be positive, yielding a bound on $v$ and $\mu$, which in turn places an upper bound on the maximum possible amplitude,

$$v<v_m=\frac{3}{4}R(A_*), \quad \mu<\frac{\varepsilon^{4/3}}{2\pi}v_m^{2/3}, \tag{33}$$

$$A_{\max}=A_*+\mu. \tag{34}$$

The eigenvalue $\lambda^1$ is given by

$$\lambda^1=-\frac{1}{A_*^2}\left[2\int_0^{A_*}M(A')\,\mathrm{d}A'+\mu\left(R(A_*)-\frac{8v}{15}\right)\right]. \tag{35}$$

Let us now suppose that the function $f(z')$ is given by

$$f(z')=\alpha_1 z'+\alpha_2 z'^2+\alpha_3 z'^3, \tag{36}$$

so that Eqs. (27), (32) and (35) yield

$$M(A)=\frac{9\pi^2}{4}\alpha_3 A^3+8\pi\left(\alpha_3+\frac{2}{3}\alpha_2\right)A^2, \tag{37}$$

$$R(A_*)=\frac{9\pi^2}{4}\alpha_3 A_*^3+\frac{16\pi}{3}\left(\alpha_3+\frac{2}{3}\alpha_2\right)A_*^2, \tag{38}$$

$$\lambda^1=-\left(\frac{32}{9}\alpha_2+\frac{155}{24}\alpha_3\right)\pi A_{\max}-\frac{9\pi}{8}\alpha_3\mu+\frac{2}{15}\frac{(2\pi)^{7/2}}{\varepsilon^2}\mu^{5/2}, \tag{39}$$

where $\alpha_1$ is chosen conveniently to remove the linear term in $M(A)$ so that

$$\alpha_1=-\alpha_2-\left(1-\frac{3}{2\pi^2}\right)\alpha_3. \tag{40}$$

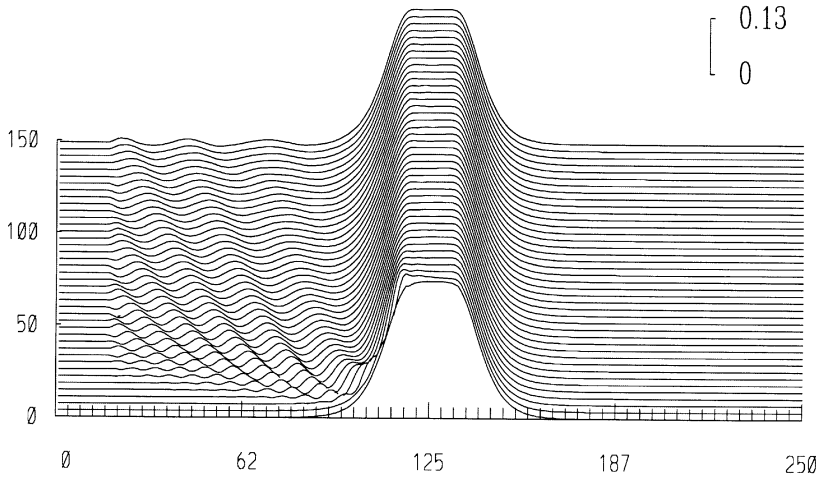


Fig. 1. Time evolution of density at depth $\frac{2}{3}h$ for $\mu = 0.95\mu_{\max}$, $\sigma = 0.01$, $\alpha_3 = 1$ and $\alpha_2 = -1.5$ (mKdV outer solution).

Introducing $\kappa^2 = -\lambda^1$ Eq. (28) becomes

$$A_X^2 - \kappa^2 A^2 + \tau_1 A^3 + \tau_2 A^4 = 0, \tag{41}$$

where

$$\tau_1 = \frac{16\pi}{3}\left(\alpha_3 + \frac{2}{3}\alpha_2\right) \quad \text{and} \quad \tau_2 = \frac{9\pi^2}{8}\alpha_3. \tag{42}$$

Let us consider the two cases $\alpha_3 = 0$ or $\alpha_2 = -\frac{3}{2}\alpha_3$, such that $\tau_2 = 0$ or $\tau_1 = 0$, in order to remove the quartic and cubic term in the amplitude equation (41) respectively (Fig. 1).

(i) For $\alpha_3 = 0$ ($\tau_2 = 0$) Eq. (41) is the familiar steady-state Korteweg–de Vries equation (KdV) equation, which has the solution

$$A = \frac{\kappa^2}{\tau_1}\operatorname{sech}^2\frac{\kappa}{2}(|X| - X_*). \tag{43}$$

(ii) For $\alpha_2 = -\frac{3}{2}\alpha_3$ ($\tau_1 = 0$) Eq. (41) reduces to the steady modified Korteweg–de Vries (mKdV) equation

$$A_X^2 - \kappa^2 A^2 + \tau_2 A^4 = 0, \tag{44}$$

which has the positive solution

$$A = \frac{\kappa}{\sqrt{\tau_2}}\operatorname{sech}\kappa(|X| - X_*), \tag{45}$$

representing a wave of depression ($A > 0$).

The streamfunction field $\phi$ and its first derivatives have to be continuous at the vortex core boundary to ensure the continuity of the normal velocity and pressure there. The condition on $X_*$

satisfying this without any approximation is

$$X_* = |X_0| - \frac{2}{\kappa}\ln\left(\kappa\sqrt{\frac{\pi}{\tau_1}} + \sqrt{\kappa^2\frac{\pi}{\tau_1} - 1}\right) \quad \text{for } \tau_2 = 0 \tag{46}$$

and

$$X_* = |X_0| - \frac{1}{\kappa}\ln\left(\kappa\frac{\pi}{\sqrt{\tau_2}} + \sqrt{\kappa^2\frac{\pi^2}{\tau_2} - 1}\right) \quad \text{for } \tau_1 = 0. \tag{47}$$

The phase speed of the solitary waves is determined by the eigenvalue $\lambda^1$ (see Eqs. (16) and (22)) and is a function of wave amplitude, unlike the linear phase speed, which depends only on the stratification and depth of the fluid

$$c_0 = \sqrt{\sigma g h}/\pi.$$

To leading order the nonlinear phase speed can be written as

$$c = c_0\left(1 - \frac{\varepsilon^2}{2\pi^2}\lambda^1 + \mathrm{O}(\varepsilon^4)\right). \tag{48}$$

For $\tau_2 = 0$, corresponding to the KdV outer solution, the eigenvalue $\lambda^1$ given by (39) with $\alpha_3 = 0$ is

$$\lambda^1 = -\tau_1 A_{\max} + \frac{2}{15}\frac{(2\pi)^{7/2}}{\varepsilon^2}\mu^{5/2}. \tag{49}$$

If the recirculation region is absent Eq. (43) with $X_* = 0$ represents the solution over the entire domain. The eigenvalue $\lambda^1$ is given by

$$A_{\max} = \kappa^2/\tau_1, \tag{50}$$

where, since $\lambda^1 = -\kappa^2$,

$$\lambda^1_{\mathrm{KdV}} = -\tau_1 A_{\max}. \tag{51}$$

Dropping the $\mathrm{O}(\varepsilon^4)$ term subsequently, the phase speed of the solution with the recirculating region can be expressed as

$$c_{\mathrm{GD}}|_{\tau_2=0} = c_{\mathrm{KdV}} - \frac{c_0}{\pi^2}\frac{(2\pi)^{7/2}}{15}\mu^{5/2}, \tag{52}$$

where

$$c_{\mathrm{KdV}} = c_0\left(1 + \frac{\varepsilon^2}{2\pi^2}\tau_1 A_{\max}\right), \tag{53}$$

is the phase speed of the KdV solution without the recirculating region. Note that $c_{\mathrm{KdV}}$ increases with amplitude $A_{\max}$.

For $\tau_1 = 0$, the mKdV outer solution, $\lambda^1$ becomes

$$\lambda^1 = -\tau_2\frac{1}{\pi}(A_{\max} + \mu) + \frac{2}{15}\frac{(2\pi)^{7/2}}{\varepsilon^2}\mu^{5/2}. \tag{54}$$

Similarly if the recirculation region is absent Eq. (44) is the amplitude equation for the entire domain and its eigenvalue $\lambda^1$ can be computed from

$$A_{\max} = \kappa/\sqrt{\tau_2}, \tag{55}$$

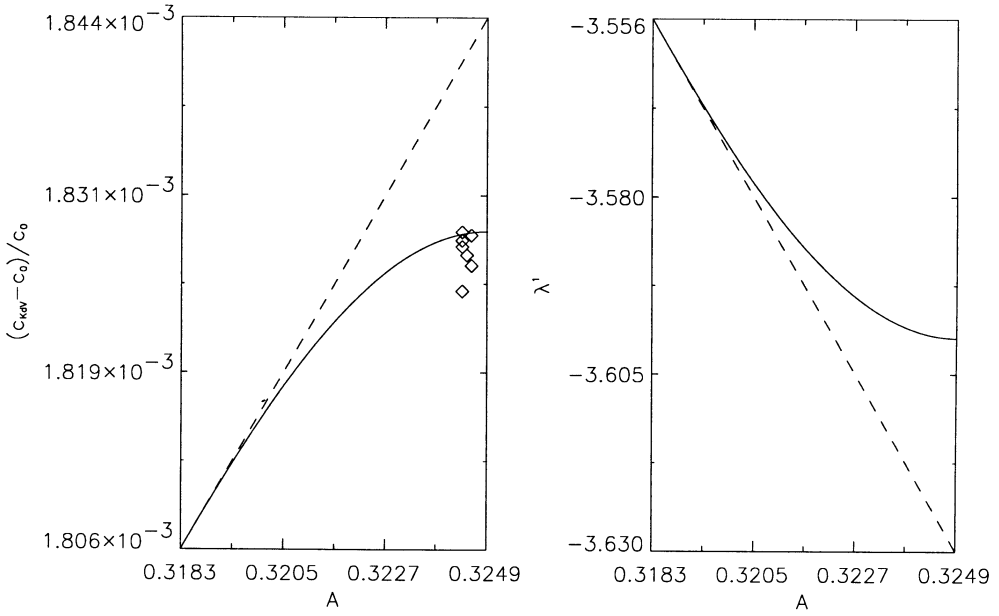


Fig. 2. Relative phase speed $(c - c_0)/c_0$ and eigenvalue $\lambda^1$ for the KdV outer solution (bold) and KdV (dashed) solution for $1/\pi \leqslant A_{\max} < 1/\pi + \mu_{\max}$, diamonds denote the numerical results.

yielding

$$\lambda^1_{\mathrm{mKdV}} = -\tau_2 A^2_{\max} \tag{56}$$

for the eigenvalue and

$$c_{\mathrm{mKdV}} = c_0 \left(1 + \frac{\varepsilon^2}{2\pi^2}\tau_2 A^2_{\max}\right) \tag{57}$$

for the phase speed. Note that the phasespeed of the mKdV solution increases with $A^2_{\max}$ in contrast to the KdV solution which increases with $A_{\max}$ only. The phase speed of the solution with the incorporated recirculation region is

$$c_{\mathrm{GD}}|_{\tau_1=0} = c_0 \left(1 + \frac{\varepsilon^2}{2\pi^2}\tau_2 \frac{1}{\pi}(A_{\max} + \mu) - \frac{c_0}{\pi^2}\frac{(2\pi)^{7/2}}{15}\mu^{5/2}\right). \tag{58}$$

The relative phase speed

$$(c_{\mathrm{GD}} - c_0)/c_0$$

for the two outer solutions considered is plotted in Figs. 2 and 3. The GD solution is of the order $\mathrm{O}(10^{-3})$ and $\mathrm{O}(10^{-2})$ slower than the phase speed of the KdV and mKdV solution, for the KdV and mKdV outer solution, respectively. The GD solution is also faster than the speed of the linear long wave (see Eq. (53)). The width of the initial streamfunction field increases with amplitude (Fig. 4). Note that in the KdV case $\lambda^1 = -\tau_1/\pi + \mathrm{O}(\mu)$, and in the mKdV case $\lambda^1 = -\tau_2/\pi^2 + \mathrm{O}(\mu)$.

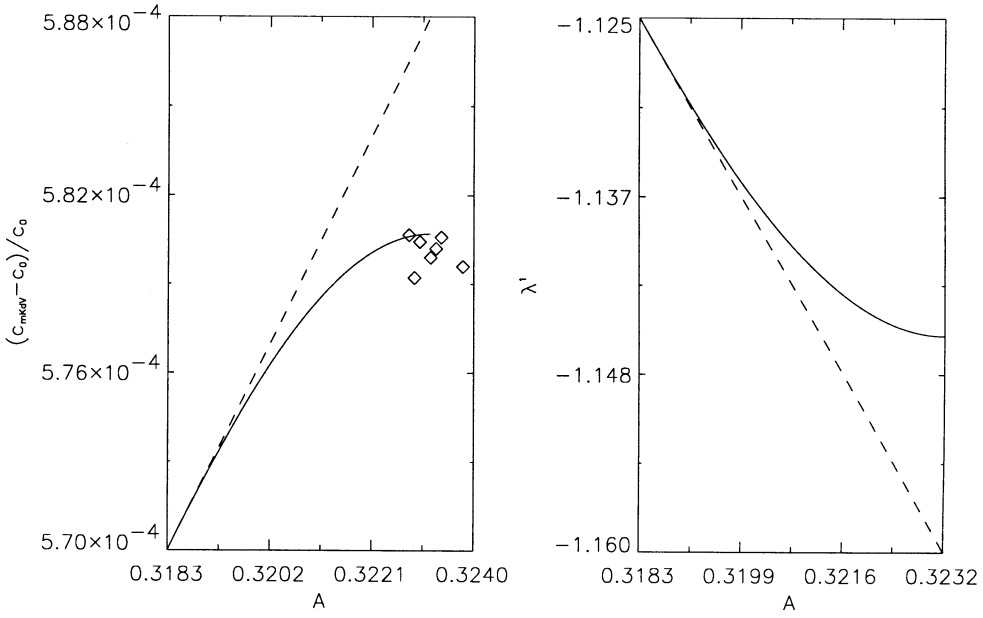


Fig. 3. Relative phase speed $(c - c_0)/c_0$ and eigenvalue $\lambda^1$ of the DG for the mKdV outer solution (bold) and mKdV (dashed) solution for $1/\pi \leqslant A_{\max} < 1/\pi + \mu_{\max}$, diamonds denote the numerical results.

Thus in both cases $X_* - |X_0|$ is $O(\mu^{1/2})$, which is required for consistency with the scaling for the inner region.

## 4. Numerical results

To test the validity of the preceeding asymptotic theory we consider some numerical simulations of the unsteady Eqs. (1)–(4). Since solitary waves conserve momentum and energy it is of vital importance for the numerical scheme to be nondissipative, more precisely that the nonlinear convective term in the governing equation is represented in conservative form (Zang, 1990). Applying the Boussinesq approximation to the vector form of the momentum equation yields

$$\boldsymbol{u}_t + (\boldsymbol{u} \cdot \nabla)\boldsymbol{u} = -\frac{1}{\rho_0}\nabla p - \frac{\rho g}{\rho_0}\boldsymbol{k}. \tag{59}$$

Taking the curl of Eq. (59) yields an equation for the vorticity $\boldsymbol{\zeta} = \nabla \times \boldsymbol{u}$,

$$\boldsymbol{\zeta}_t - \nabla \times (\boldsymbol{u} \times \boldsymbol{\zeta}) = -\frac{\rho_x}{\rho_0} g\boldsymbol{j}, \tag{60}$$

Since the flow is two dimensional, the vorticity vector $\boldsymbol{\zeta}$ has only one component in the $y$-direction $\boldsymbol{\zeta} = \zeta \boldsymbol{j}$ and so Eq. (60) reduces to

$$\frac{\mathrm{d}\zeta}{\mathrm{d}t} = -\frac{\rho_x}{\rho_0} g. \tag{61}$$

Thus vorticity can only be generated by a nonzero horizontal density gradient.

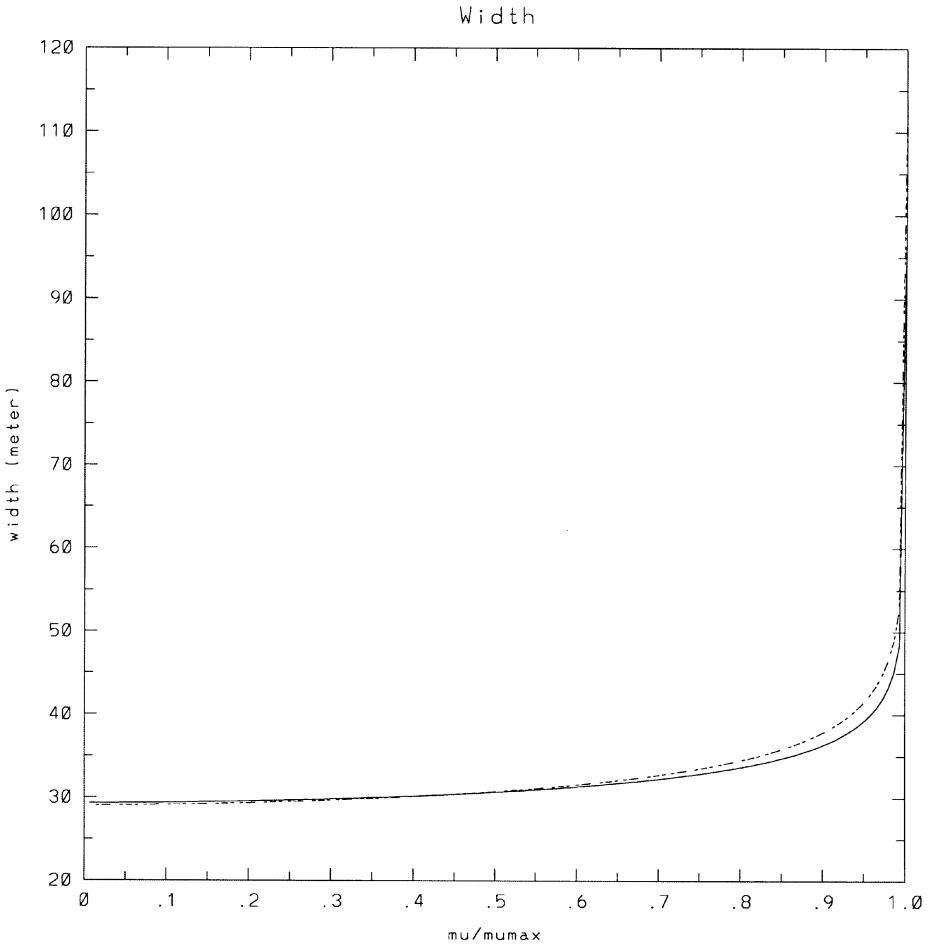


Fig. 4. Plot of the width for $0 < \mu < \mu_{\max}$ for the KdV (bold) and mKdV (dashed) outer solution ($\alpha_2 = 1$ and $\alpha_3 = 1$ resp.)

Consider a perturbation to the basic density field

$$\rho(x,z) = \bar{\rho}(z) + \rho'(x,z), \tag{62}$$

then the vorticity equation (60) and density equation (3) become

$$\zeta_t = -\nabla \cdot (\boldsymbol{u}\zeta) - \sigma_x^*, \tag{63}$$

$$\sigma_t^* = -\nabla \cdot (\boldsymbol{u}\sigma^*) + w \cdot N^2, \tag{64}$$

where the Brunt-Väisälä frequency is given by

$$N^2(z) = -g\frac{1}{\rho_0}\frac{\mathrm{d}\bar{\rho}}{\mathrm{d}z} \tag{65}$$

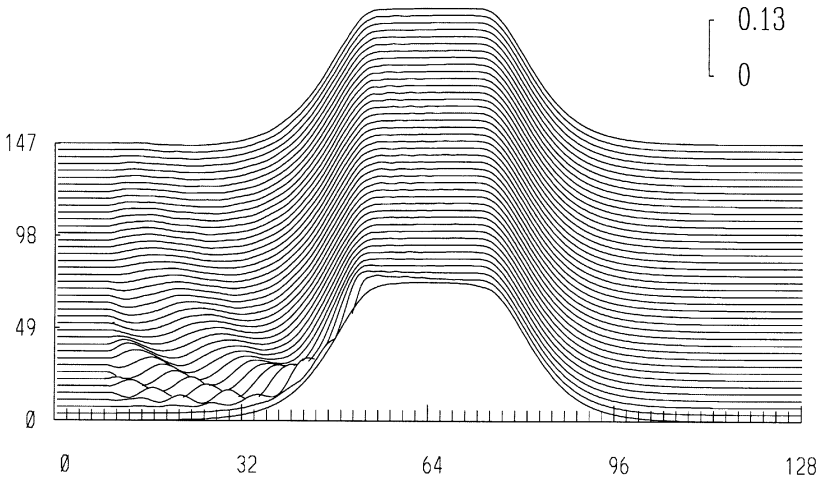


Fig. 5. Time evolution of density at depth $\frac{2}{3}h$ for $\mu = 0.95\mu_{\max}$, $\sigma = 0.01$, $\alpha_2 = 1$ and $\alpha_3 = 0$ (KdV outer solution).

and

$$\sigma^* = g\rho'/\rho_0. \tag{66}$$

Eqs. (63) and (64) are the equations which are integrated numerically; the nonlinear convective term is computed in an energy conserving form. The spectral numerical scheme used here has been successfully employed by Rottman et al. (1996) to study the unsteady flow of an incompressible, inviscid Boussinesq flow over topography. It employs Chebyshev collocation in the vertical and Fourier modes in the horizontal and uses a fourth-order standard Runge–Kutta scheme for timestepping. To resolve the recirculation region a resolution of $256 \times 65$ is used in the following. A 2/3 filter on the highest modes is used to remove aliasing errors and a sponge is situated across the periodic boundary condition in the horizontal to prevent energy propagated downstream from re-entering the domain.

Time is normalized with twice the halfwidth $D = 2(x_0 + \bar{x})$ and the phase speed $c$. A measure of the width of the outer region being $\bar{x} = 2/\varepsilon\kappa$ for case (i) and $\bar{x} = 1/\varepsilon\kappa$ for case (ii), these being the KdV and mKdV cases in the outer region, respectively, while $x_0$ represents the halfwidth of the inner region where Eq. (30) is valid. The stratification parameter $\sigma$ is set to $\sigma = 0.01$ in the following to satisfy the Boussinesq approximation.

The KdV solution was tested first and remained of permanent form, satisfying the first three conservation laws to first order.

For the initialization of the streamfunction field in the inner region the first term of an expansion in powers of $\xi^2$ is used to approximate the bounded solution to Eq. (30) near $B = 1$,

$$B = 1 - k\xi^2, \quad \text{where } k = \tfrac{1}{4}R(A_*) - \tfrac{1}{3}v. \tag{67}$$

Notice that the bound on $v$ (33) appears as the coefficient of the first term in this expansion. A standard fourth-order Runge–Kutta solver continues the solution to $B = 0$, determining the width of the inner region. Initially the streamfunction is set to a constant, $\phi = \phi(1)$, inside the recirculation region and the discontinuity of $\phi_z$ is smoothed. The initial density field is calculated taking advantage of Eqs. (7) and(9) together with Eq. (14).

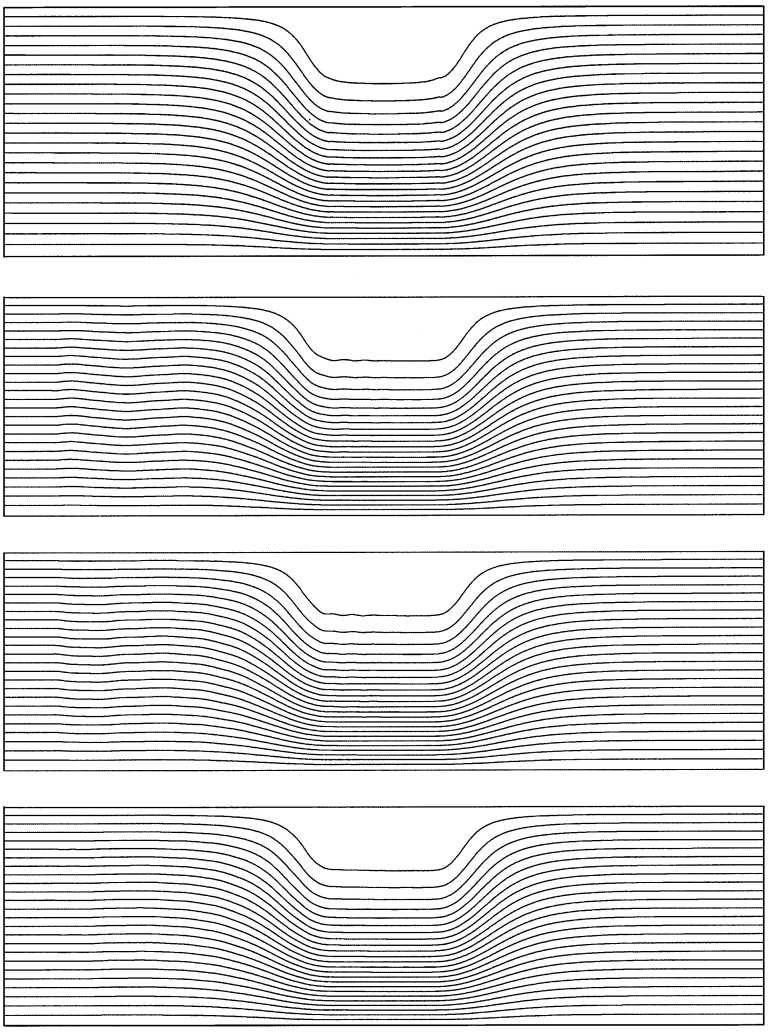

Fig. 6. Density plots for normalized times $t_n = 0, 69.89, 106.67$ and 147.13.

The numerical results for both the KdV and mKdV outer solutions show that the approximate initial conditions shed transients (Figs. 5, 6 and 9, 10), which propagate downstream only (see also Fig. 1). Permanent steady solitary waves evolve after the flow has traversed the width of the waves for more than a hundred times, indicating the steady state of the solutions. In the close-up contours of the recirculation regions the streamfunction fields remain homogeneous (Figs. 7 and 11 ), whereas the density field shows density inversions of higher order (i.e. variability of $O(10^{-6})$), but remains homogeneous to first order as predicted by DG. As a measure of the strength of the closed streamline region the maximum horizontal velocity opposing the downstream flow is measured at the top of the recirculation region. This adverse velocity opposing the flow at the upper boundary is of second order (Figs. 8 and 12). The adverse velocity of the solution with the KdV outer solution decays to a level which cannot be resolved numerically. In contrast the adverse velocity of the solution with

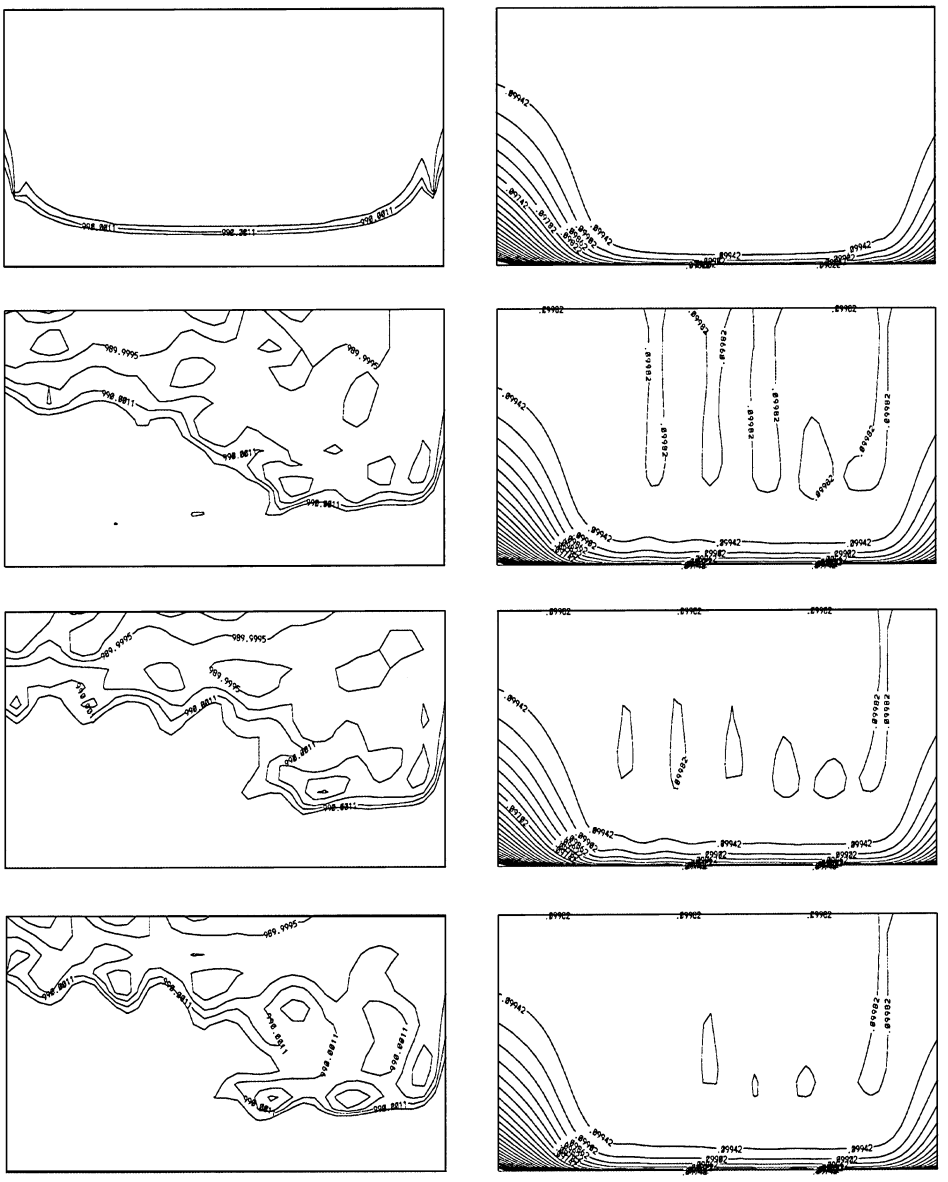

Fig. 7. Plot of density (left) and streamfunction (right) for normalized times $t_n = 0, 69.89, 106.67$ and 147.13 inside of the recirculation region, $41 \times 23$ grid points resolution for $\rho$ and $61 \times 23$ grid points for $\psi$.

the mKdV outer solution approaches a positive value. The results show that the recirculation region is stagnant to first order, as predicted by the asymptotic analysis of Derzho and Grimshaw.

The amplitude of the steady-state solution is measured for a number of different phase speeds from $0.65\mu_{\max}$ to $0.95\mu_{\max}$, denoted by diamonds in Figs. 2 and 3. The results agree with the theoretical results for the amplitude-phase speed relations to within the error of the computation.

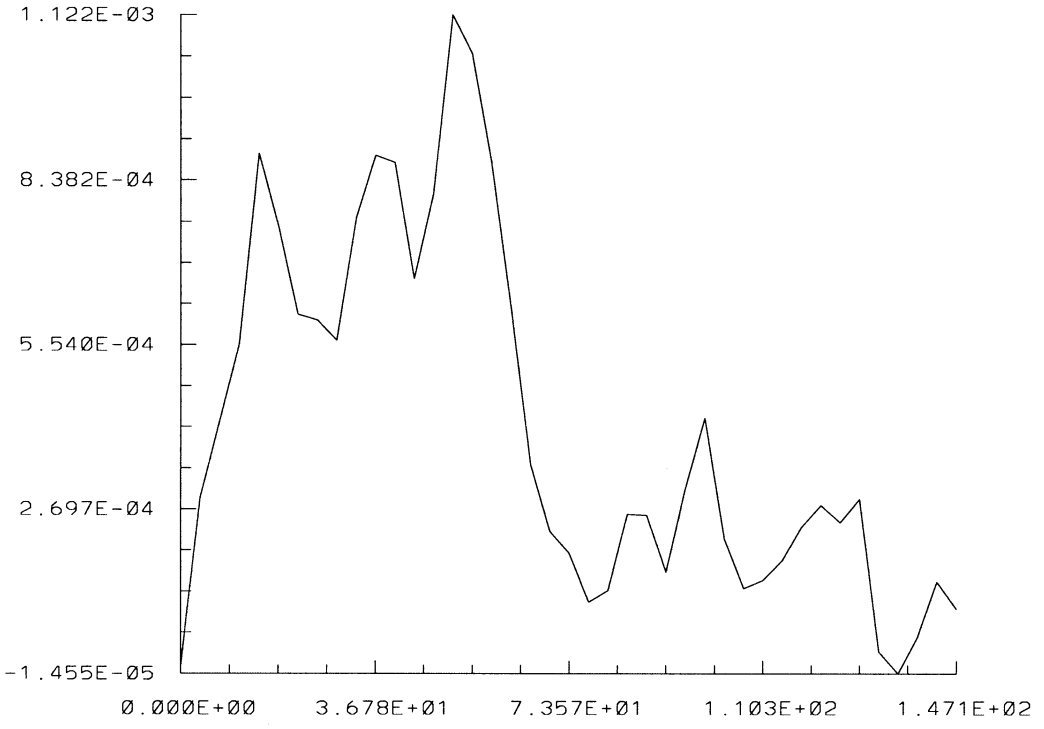


Fig. 8. Maximum adverse velocity $u$ at the upper boundary.

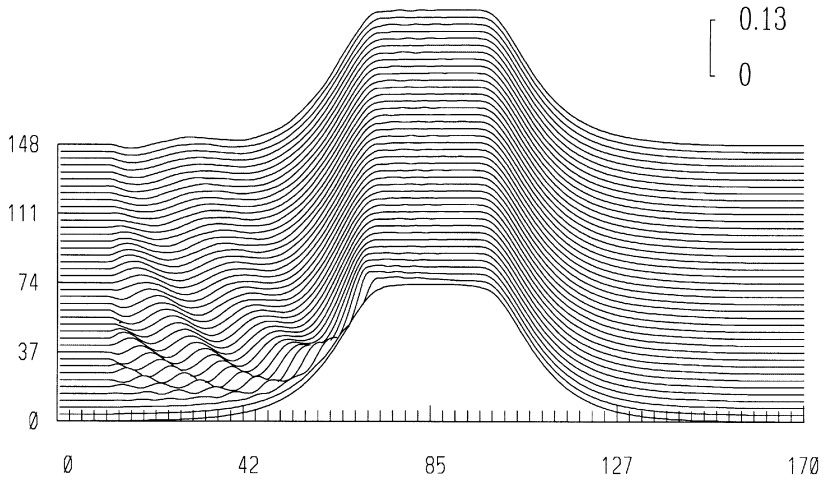


Fig. 9. Time evolution of density at depth $\frac{2}{3}h$ for $\mu = 0.95\mu_{\max}$, $\sigma = 0.01$, $\alpha_2 = -1.5$ and $\alpha_3 = 1$ (mKdV outer solution).

## 5. Conclusion

The solitary waves in a weakly stratified shallow fluid studied in this paper proved to be stable and of permanent shape. The solutions possess the characteristics of large amplitude solitary

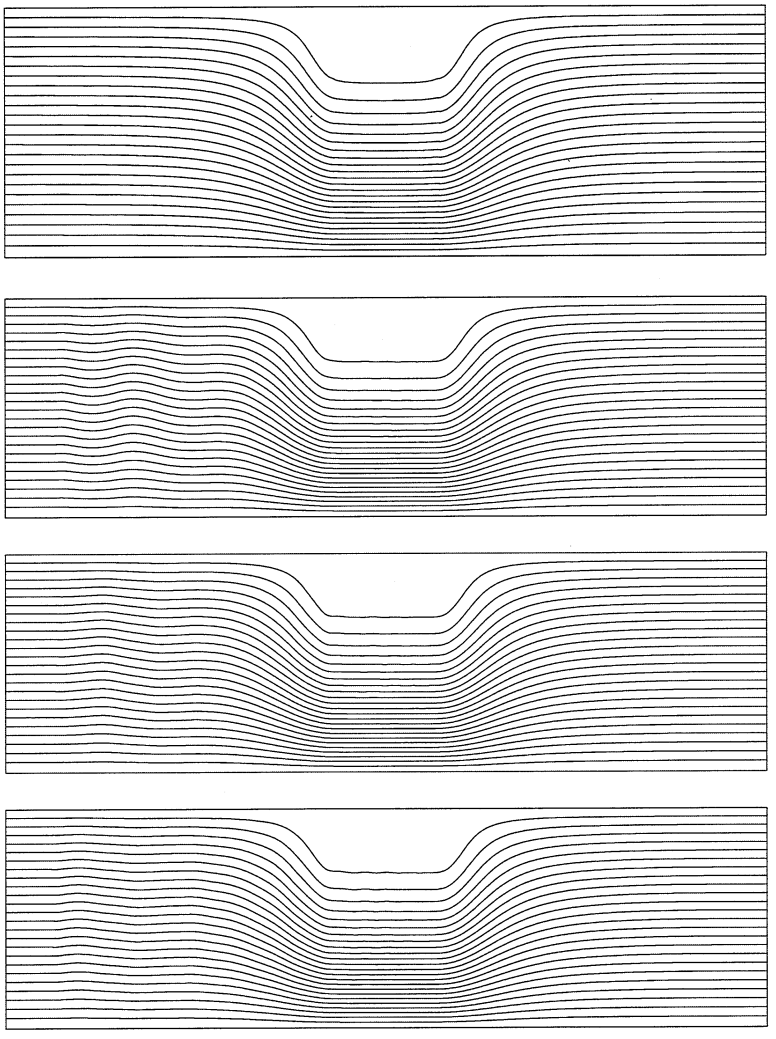

Fig. 10. Density plots for normalized times $t_n = 0, 70.24, 107.21$ and 147.88.

waves. The width increases with amplitude and the phase speed depends nonlinearly on the amplitude ($\mu = A_{\max} - A_*$). The width of the solutions tends to infinity for the maximum possible amplitude ($\mu \to \mu_{\max}$), indicating the termination of this asymptotic theory. The results show that solitary waves with an essentially homogeneous vortex core exist in a Boussinesq fluid. The amplitude is in both cases governed by the nonlinear equations (26) and (30) (cf. Derzho and Grimshaw, 1997).

The recent laboratory experiments by Stamp and Jacka (1995) of solitary waves with vortex cores, which were generated by displacing a very large mass of fluid along a very thin thermocline, generally support the theoretical and numerical results presented here, but seem to show that considerable mass is transported with the wave. This was not the case here, instead our results indicate that the

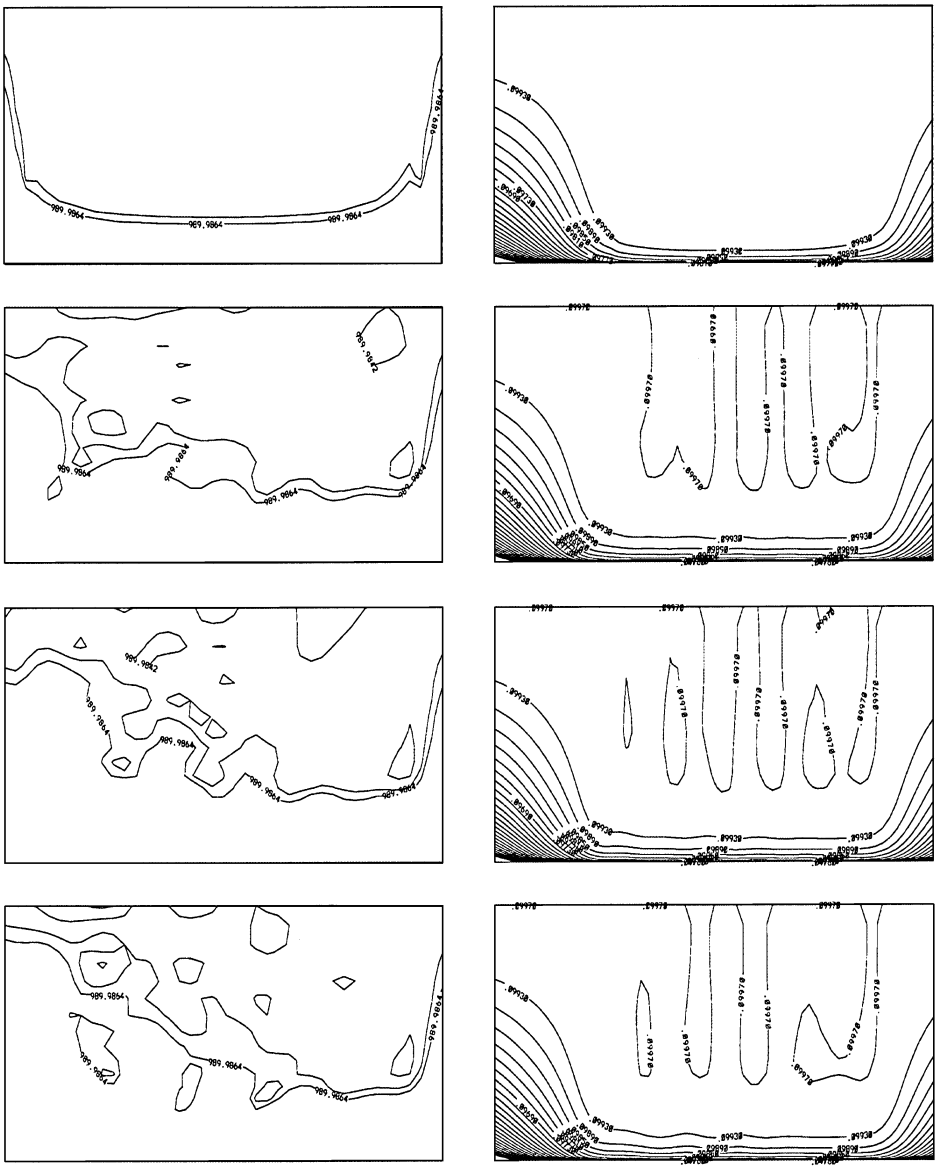

Fig. 11. Plot of density (left) and streamfunction (right) for normalized times $t_n = 0, 70.24, 107.21$ and 147.88 inside of the recirculation region, $41 \times 23$ grid points resolution for $\rho$ and $61 \times 23$ grid points for $\psi$.

steady state tends to be a solitary wave with a vortex core carrying only little mass. The numerical simulation by Terez and Knio (1998) of the gravitational collapse of a mixed region along a thermocline produced similar solitary waves with vortex cores of diminishing mass, which is in better agreement with our results.

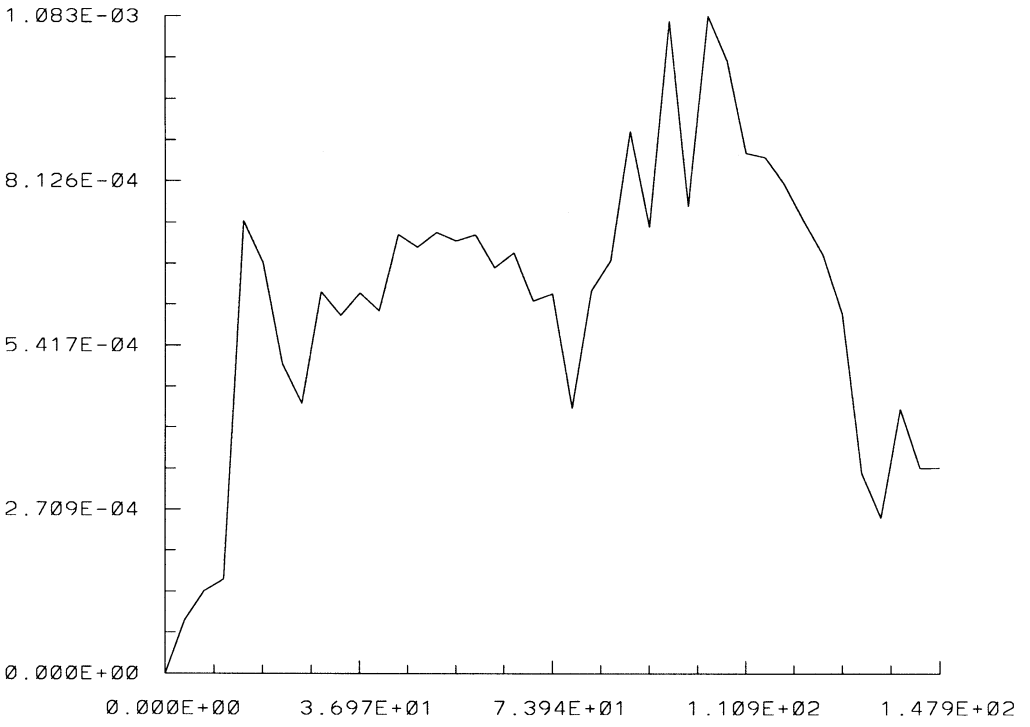


Fig. 12. Maximum adverse velocity $u$ at the upper boundary.

## References

Benney, D.J., Ko, D.R.S., 1978. The propagation of long large amplitude internal waves. Stud. Appl. Math. 59, 187–199.

Derzho, O.G., Grimshaw, R., 1997. Solitary waves with a vortex core in a shallow layer of stratified fluid. Phys. Fluids 9 (11), 3378–3385.

Dubreil-Jacotin, M.L., 1937. Sur la determination rigoureuse des ondes permanentes periodiques d'amplitude finite. J. Math. Pure Appl. 13, 217.

Gear, J.A., Grimshaw, R., 1983. A second-order theory for solitary waves in shallow fluids. Phys. Fluids 26 (1), 14–29.

Grimshaw, R., 1980/81. Solitary waves in compressible fluid. J. Pure Appl. Geophys. 119, 780–797.

Grimshaw, R., 1997. Internal solitary waves. In: Liu, P.L.-F. (Ed.), Advances in Coastal and Ocean Engineering. World Scientific, Singapore, vol. 3, pp. 1–30.

Grimshaw, R., Yi, Z., 1991. Resonant generation of finite-amplitude waves by the flow of a uniformly stratified fluid over topography. J. Fluid Mech. 229, 603–628.

Chan, T.F., Tung, K.-K., Kubota, T., 1982. Large amplitude internal waves of permanent form. Stud. Appl. Math. 66, 1–44.

Leonov, A.I., Miropol'skiy, Yu.Z., 1975. Toward a theory of stationary nonlinear internal gravity waves. Atmos. Ocean. Phys. 11, 298–304.

Long, R.R., 1953. Some aspects of the flow of stratified fluids. I. A theoretical investigation. Tellus 5, 42.

Long, R.R., Morton, J.B., 1966. Solitary waves in compressible, stratified fluids. Tellus XVIII 1, 79–85.

Pelinovsky, D.E., Grimshaw, R.H.J., 1997. Instability analysis of internal solitary waves in a nearly uniformly stratified fluid. Phys. Fluids 9 (11), 3343–3352.

Rottman, J.W., Broutman, D., Grimshaw, R., 1996. Numerical simulations of uniformly stratified fluid flow over topography. J. Fluid Mech. 306, 1–30.

Stamp, A.P., Jacka, M., 1995. Deep-water internal solitary waves. J. Fluid Mech. 305, 347–371.

Terez, D.E., Knio, O.M., 1998. Numerical simulations of large-amplitude internal solitary waves. J. Fluid Mech. 362, 53–82.

Zang, T.A., 1990. Spectral methods for simulations of transition and turbulence. Comp. Meth. Appl. Mech. Eng. 80, 209–221.